Acta Crystallographica Section D
Biological Crystallography
ISSN 0907-4449

A method for screening the temperature dependence of three-dimensional crystal formation

Michael J. Landsberg,[a] James Bond,[b] Christine L. Gee,[a] Jennifer L. Martin[a] and Ben Hankamer[a]*

[a]Institute for Molecular Bioscience, Queensland Biosciences Precinct, The University of Queensland, Brisbane, Queensland 4072, Australia, and [b]Eppendorf South Pacific Pty Ltd, North Ryde, NSW 2113, Australia

Correspondence e-mail: b.hankamer@imb.uq.edu.au

Received 7 October 2005
Accepted 20 February 2006

Temperature is an important parameter controlling protein crystal growth. A new temperature-screening system (Thermo-screen) is described consisting of a gradient thermocycler fitted with a special crystallization-plate adapter onto which a 192-well sitting-drop crystallization plate can be mounted (temperature range 277–372 K; maximum temperature gradient 20 K; interval precision 0.3 K). The system allows 16 different conditions to be monitored simultaneously over a range of 12 temperatures and is well suited to conduct wide (∼20 K) and fine (∼3 K) temperature-optimization screens. It can potentially aid in the determination of temperature phase diagrams and run more complex temperature-cycling experiments for seeding and crystal growth.

1. Introduction

X-ray crystallography is by far the most successful method of protein structure determination, accounting for more than 84% of the entries (∼29 000 of ∼35 000) in the Protein Data Bank (PDB; Berman *et al.*, 2000). Despite this success, the rate of protein structure determination still lags far behind the rate at which new and functionally interesting proteins are identified. Currently, over 1800 genome-sequencing projects worldwide are in progress (∼1500) or complete (335) (Bernal *et al.*, 2001) and have already yielded in excess of 3.2 million non-redundant protein sequences (Wu *et al.*, 2003). Recent high-throughput sequencing initiatives have identified an unexpectedly high proportion of novel unrelated genes (Venter *et al.*, 2004), suggesting that we have only scratched the surface with regard to genetic diversity. To keep up with this rapidly expanding set of protein sequences, structure-determination rates will have to be improved.

Obtaining large diffraction-quality crystals remains one of the single largest obstacles in protein crystallography (Wiencek, 1999). Overcoming this rate-limiting step requires the development of new strategies that improve the rate of crystal production. Techniques such as incomplete factorial screening (Carter & Carter, 1979) or sparse-matrix approaches (Jancarik & Kim, 1991) are typically used to screen the effect of solution properties on crystallization. Equally, temperature influences protein solubility (and therefore crystallization), but is rarely screened in any great detail. In the rare instances where temperature is screened in crystallization trials, it is usually at no more than two or three convenient temperatures (usually 277 and 293 K), despite the fact that many proteins have in fact been crystallized at vastly different temperatures to these (Bridgen *et al.*, 1976; Earhart *et al.*, 1993) and that subtle changes in temperature have been shown to influence protein solubility and phase formation profoundly (Bergfors, 1999; Haas & Drenth, 1998, 2000). Systems enabling the cost-effective sampling of a wider and finer temperature space would therefore provide a powerful new route to optimize the rate and quality of three-dimensional crystal production.

Here, we present a new temperature-screening system (Fig. 1) capable of covering a 277–372 K temperature range at a maximal sampling resolution of 0.3 K, together with proof-of-principle data demonstrating its capabilities (Fig. 2).

2. Experimental

Crystallization trials were set up in 384-well Corning (Acton, MA, USA) Crystal*EX* crystallization plates (to screen up to 192 conditions). Each well contained 100 µl of the appropriate reservoir solution. Chicken egg-white lysozyme (Sigma, St Louis, MO, USA; EC 3.2.1.17) was dissolved at 50 mg ml^{-1} in 10 m*M* sodium acetate pH 4.5 and equilibrated with a reservoir solution of 65 mg ml^{-1} sodium chloride, 0.1 *M* sodium acetate pH 4.5 supplemented with 0.02% sodium azide. Bovine liver catalase (Sigma; EC 1.11.1.6) was crystallized from a 30 mg ml^{-1} stock solution buffered with 25 m*M* HEPES pH 7.0 and with a reservoir solution of 1 *M* sodium acetate, 0.1 *M* imidazole pH 6.5, 0.02% sodium azide. The human adrenalin-synthesizing enzyme phenylethanolamine *N*-methyltransferase (PNMT) was expressed, purified and crystallized under conditions described previously (Gee *et al.*, 2005). Crystals formed in sitting drops consisting of either 2 µl (lysozyme and catalase) or 1 µl (PNMT) each of the protein stock and reservoir solutions.

Crystallization trays were incubated in an Eppendorf Mastercycler gradient thermocycler (Hamburg, Germany) fitted with aluminium adaptors (Thermo-screen; Fig. 1). Operation of the system is relatively straightforward, since it is used in exactly the same way as for gradient PCR. In the experiments described here, the system was programmed to run at a median value of either 285 K (all proteins) or 295 K (lysozyme only) with a gradient of ±8 K applied across the heating block. Lysozyme and catalase were incubated for 48 h, while PNMT was incubated for 11 d. Trays were imaged using a Crystal Monitor automated crystallization imaging workstation (Emerald BioSystems, Bainbridge Island, WA, USA).

3. Results

Lysozyme crystallization trials revealed a clear temperature effect on the number of crystals yielded and their size (Figs. 2*a* and 2*d*). At low temperatures (∼279 K), hundreds of small crystals were observed per drop. Increasing the incubation temperature from 279 to 292 K yielded progressively fewer crystals of increased size and quality. This observation is consistent with a direct correlation between increased temperature and solubility for lysozyme. At an optimal temperature of between 293.0 and 294.5 K (see Fig. 2*a*; 293.0 K), a few large (>0.4 mm) hexagonal crystals were observed per drop. Increasing the temperature further towards 303 K resulted in a reduction in crystal size, which could be explained either by a continued increase in protein solubility or by protein denaturation. The same temperature dependence (*i.e.* maximum crystal size at ∼293 K) was found in two independent lysozyme crystallization runs covering overlapping temperature ranges (Fig. 2*d*). This clearly demonstrates the reproducibility of the technique.

Further crystallization trials with PNMT revealed a similarly striking temperature effect (Figs. 2*b* and 2*e*); however, in this instance we identified a different optimal temperature to that for lysozyme. At lower temperatures (∼279 K), relatively few crystals were observed. The number of crystals decreased as the temperature was raised, consistent with a correlation between increasing temperature and solubility for PNMT. The 282.5–285.2 K range contained the fewest number of crystals, which as expected had the largest size (up to 0.15 mm). However, as the temperature was increased further crystal size diminished, accompanied by an increase in the number of crystals, gradually at first and then significantly from 290.6 K onward, until at 293 K only numerous small microcrystals were visible. These results suggest an optimal temperature of ∼283 K for PNMT crystallization; significantly, this temperature is different to that which we have previously used for PNMT crystallization.

The catalase crystallization trials exhibited a less clearly defined pattern, although a general temperature-dependent trend was still evident. Some temperatures did not yield crystals; of those that did, we observed three distinct crystal morphologies (Fig. 2*c*). Small needle clusters and showers were observed over the temperature ranges 279.2–282.5 K (6/16 replicates) and 286.9–288.4 K (4/16 replicates). Larger needles and rod-shaped crystals (up to 0.2 mm in length) were observed over the temperature range 292.2–293.4 K (13/16 replicates). The results suggest that the optimal temperature for catalase is ∼293 K; however, altering the buffer components may lead to improvements in crystal quality in the lower favourable temperature ranges (∼279–282 and ∼287–288 K). Further experiments are required to fully investigate this possibility. Additionally, the observation of different crystal morphologies may be attributed to the formation of different crystalline phases as the temperature changes, a hypothesis that may also support the observed decrease in size of lysozyme and PNMT crystals as the temperature is increased beyond the optima.

4. Discussion

The Thermo-screen system described here is designed to conduct protein crystallization trials at any temperature between 277 and 372 K. Fitted with a Corning 384-well crystallization plate, the system can be employed to screen an entire crystallization plate at one temperature or, utilizing the gradient function of the thermocycler, the instrument is capable of screening up to 12 different temperatures simultaneously. This configuration also allows up to 16 different buffer conditions and/or proteins to be tested at each temperature.

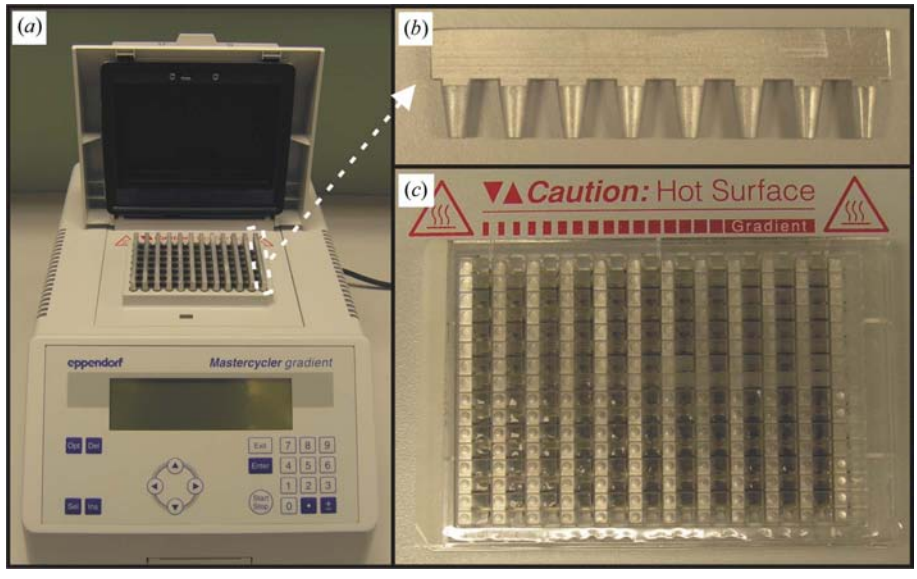

Figure 1
The Thermo-screen crystallization system. (*a*) Thermocycler, (*b*) crystallization-plate adapter, (*c*) crystallization tray mounted in thermocycler.

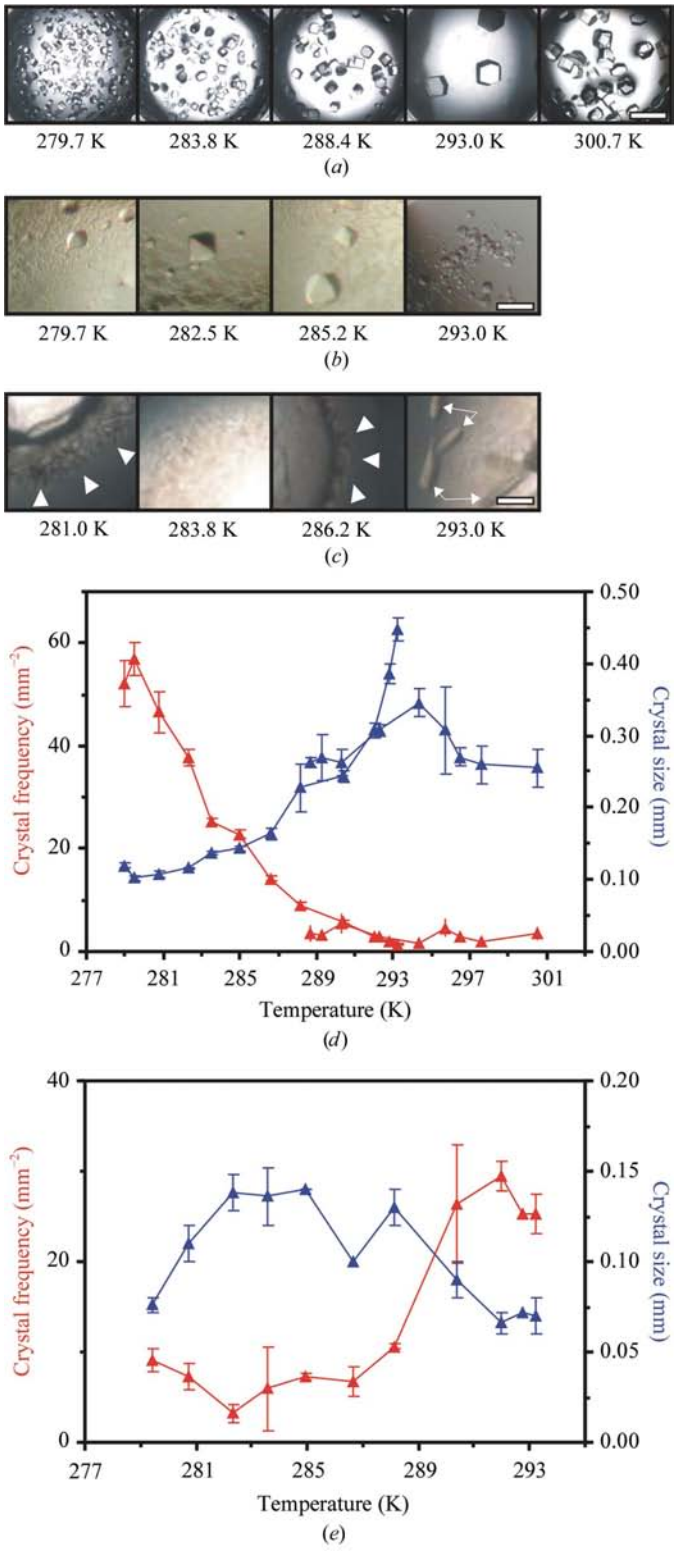

Figure 2
The effect of temperature on crystallization. Representative images of (*a*) lysozyme crystals (scale bar = 500 µm), (*b*) PNMT crystals (scale bar = 125 µm) and (*c*) catalase crystals (scale bar = 120 µm) are shown. In (*c*), small needles (arrowheads) and rods (arrows) are indicated. The effect of temperature on the number of crystals observed (red) and crystal size (blue) is shown for lysozyme (*d*) and PNMT (*e*). Crystal size was defined by the shortest axis of the largest crystal in each drop. The number of crystals is represented as the number per mm^2. Error bars are the standard error of the mean. Error bars which are not visible are smaller than the height of the data point. For the lysozyme buffer system, not all wells from the higher temperature screen could be imaged owing to excessive evaporation.

The use of a broad gradient enables a wide temperature range (up to 20 K) to be screened in a single experiment. However, even small changes in temperature can drastically affect the solubility of proteins. For example, lysozyme is reported to exhibit significant changes in solubility over a ΔT of as low as 0.5 K (Haas & Drenth, 1998, 2000) and for this reason precise refinement of crystallization temperature may be desirable for some proteins. Our temperature precision measurements (data not shown) indicate that in the present configuration this machine can routinely operate at a ΔT of 0.3 K between adjacent wells.

We have demonstrated here the effectiveness of this system with three test proteins and discovered that under the selected crystallization conditions the optimal protein crystallization temperature for lysozyme is between 293.0 and 294.5 K and that PNMT and catalase yield optimal crystals over the temperature ranges 282.5–285.2 and 292.2–293.4 K, respectively. The identification of an optimal temperature for PNMT different to that routinely used for crystallization (293 K) is particularly pertinent given that this may not have been otherwise identified. Furthermore, we have demonstrated proof-of-principle that incubation temperature affects protein crystal formation and that using the system described in this paper this effect can be successfully, conveniently and cost-effectively screened to identify optimal temperatures for protein crystallization experiments.

Finally, the Thermo-screen system is well equipped to handle advanced crystallization studies. It has previously been demonstrated that the accurate determination of phase diagrams for a protein can greatly increase the probability of obtaining high-quality protein crystals suitable for structure determination (Asherie, 2004; Saridakis & Chayen, 2003). The ability to screen up to 192 crystallization conditions (16 buffer conditions at 12 different temperatures) allows the rapid determination of such phase diagrams. Furthermore, the Thermo-screen system, like all modern thermocyclers, is capable of carrying out pre-programmed temperature changes during incubation. From a crystallization perspective, this is convenient as 'dynamic temperature control' has previously yielded crystals of several proteins (Cutfield *et al.*, 1974; King, 1965; Pullen *et al.*, 1975; Rose *et al.*, 1988). In addition, more subtle changes in temperature have also been credited with yielding crystals of increased size and quality (Baker & Dodson, 1970). For example, it is thought that following nucleation the temperature can be raised to dissolve smaller crystals, forming a supersaturated solution upon cooling, under which conditions the few remaining large crystals are induced to grow to a larger size and higher quality (Baker & Dodson, 1970). The system we have described in this communication allows such temperature-ramping experiments to be carried out routinely and in a fully automated manner.

The authors would like to acknowledge the SRC for Functional and Applied Genomics (University of Queensland) for providing us with crystallization screening facilities.

References

Asherie, N. (2004). *Methods*, **34**, 266–272.
Baker, E. N. & Dodson, G. (1970). *J. Mol. Biol.* **54**, 605–609.
Bergfors, T. (1999). Editor. *Protein Crystallization: Techniques, Strategies and Tips*, pp. 29–38. La Jolla: International University Line.
Berman, H. M., Westbrook, J., Feng, Z., Gilliland, G., Bhat, T. N., Weissig, H., Shindyalov, I. N. & Bourne, P. E. (2000). *Nucleic Acids Res.* **28**, 235–242.
Bernal, A., Ear, U. & Kyrpides, N. (2001). *Nucleic Acids Res.* **29**, 126–127.
Bridgen, J., Harris, J. I. & Kolb, E. (1976). *J. Mol. Biol.* **105**, 333–335.
Carter, C. W. & Carter, C. W. (1979). *J. Biol. Chem.* **254**, 2219–2223.

Cutfield, J. F., Cutfield, S. M., Dodson, E. J., Dodson, G. G. & Sabesan, M. N. (1974). *J. Mol. Biol.* **87**, 23–30.
Earhart, C. A., Prasad, G. S., Murray, D. L., Novick, R. P., Schlievert, P. M. & Ohlendorf, D. H. (1993). *Proteins*, **17**, 329–334.
Gee, C. L., Nourse, A., Hsin, A. Y., Wu, Q., Tyndall, J. D., Grunewald, G. L., McLeish, M. J. & Martin, J. L. (2005). *Biochem. Biophys. Acta*, **1750**, 82–92.
Haas, C. & Drenth, J. (1998). *J. Phys. Chem. B*, **102**, 4226–4232.
Haas, C. & Drenth, J. (2000). *J. Phys. Chem. B*, **104**, 368–377.
Jancarik, J. & Kim, S.-H. (1991). *J. Appl. Cryst.* **24**, 409–411.
King, M. V. (1965). *J. Mol. Biol.* **11**, 549–561.
Pullen, R. A., Jenkins, J. A., Tickle, I. J., Wood, S. P. & Blundell, T. L. (1975). *Mol. Cell. Biochem.* **8**, 5–20.
Rose, J. P., Yang, D., Yoo, C. S., Sax, M., Breslow, E. & Wang, B.-C. (1988). *Eur. J. Biochem.* **174**, 145–147.
Saridakis, E. & Chayen, N. E. (2003). *Biophys. J.* **84**, 1218–1222.
Venter, J. C. *et al.* (2004). *Science*, **304**, 66–74.
Wiencek, J. M. (1999). *Annu. Rev. Biomed. Eng.* **1**, 505–534.
Wu, C. H., Yeh, L. L.., Huang, H., Arminski, L., Castro-Alvear, J., Chen, Y., Hu, Z., Kourtesis, P., Ledley, R. S., Suzek, B. E., Vinayaka, C. R., Zhang, J. & Barker, W. C. (2003). *Nucleic Acids Res.* **31**, 345–347.